Biosensors and Bioelectronics 24 (2009) 3019–3024

Contents lists available at ScienceDirect

Biosensors and Bioelectronics

journal homepage: www.elsevier.com/locate/bios

Poly-silicon nanowire field-effect transistor for ultrasensitive and label-free detection of pathogenic avian influenza DNA

Chih-Heng Lin[a], Cheng-Hsiung Hung[b], Cheng-Yun Hsiao[a], Horng-Chih Lin[b], Fu-Hsiang Ko[c], Yuh-Shyong Yang[a,d,*]

[a] Institute of Biological Science and Technology, National Chiao Tung University, Hsinchu 300, Taiwan
[b] Institute of Electronics, National Chiao Tung University, Hsinchu 300, Taiwan
[c] Institute of Nanotechnology, National Chiao Tung University, Hsinchu 300, Taiwan
[d] Instrument Technology Research Center and National Nano Device Laboratories, NARL, Hsinchu 300, Taiwan

ARTICLE INFO

Article history:
Received 30 November 2008
Received in revised form 8 March 2009
Accepted 10 March 2009
Available online 21 March 2009

Keywords:
Poly-crystalline silicon nanowire
field-effect transistor (poly-SiNW FET)
Ultrasensitive
Label-free
Avian influenza (AI)
Biosensor

ABSTRACT

Enhanced surveillance of influenza requires rapid, robust, and inexpensive analytical techniques capable of providing a detailed analysis of influenza virus strains. Functionalized poly-crystalline silicon nanowire field-effect transistor (poly-SiNW FET) was demonstrated to achieve specific and ultrasensitive (at fM level) detection of high pathogenic strain virus (H5 and H7) DNA of avian influenza (AI) which is an important infectious disease and has an immediate need for surveillance. The poly-SiNW FET was prepared by a simple and low-cost method that is compatible with current commercial semiconductor process without expensive E-beam lithography tools for large-scale production. Specific electric changes were observed for AI virus DNA sensing when nanowire surface of poly-SiNW FET was modified with complementary captured DNA probe and target DNA (H5) at fM to pM range could be distinguished. With its excellent electric properties and potential for mass commercial production, poly-SiNW FET can be developed to become a portable biosensor for field use and point-of-care diagnoses.

1. Introduction

Global surveillance of influenza is critical for improvements in disease management and is especially important for early detection, rapid intervention, and a possible reduction of the impact of an influenza pandemic. Influenza viruses continue to be a major cause of respiratory tract infection, resulting in significant morbidity, mortality and financial burden. Avian influenza (AI), a type A virus, which causes disease in both human and poultry is subtyped according to the antigenic subtype of the hemagglutinin (HA) and neuraminidase (NA) glycoproteins. Avian influenza virus (AIV) is categorized into two groups based on their virulence. Infections of poultry with highly pathogenic avian influenza (HPAI) virus, almost always H5 or H7 subtypes, result in very high mortalities approaching 100%, whereas infections with low pathogenic strains are less severe (Deregt et al., 2006). The first case of human infection with H5N1 HPAI virus was reported in Hong Kong in 1997, and 318 human cases of avian influenza A virus infection including 192 deaths were reported to WHO from 2003 to 2007 (Tsuda et al., 2007). A pandemic may happen when the virus incorporates a novel HA gene and includes the ability to spread efficiently among humans in a population which lacks immunity to the virus.

Commonly used methods of identification of AIV include direct antigen detection, isolation in cell culture, or identification of influenza-specific RNA by reverse transcriptase-polymerase chain reaction (RT-PCR) (Wu et al., 2008). Traditional methods are generally effective but involve labor-intensive and highly trained personnel (Lodes et al., 2006). A real-time RT-PCR that can provide results on AI identification within 3 h have been developed (Durham, 2003). However, these PCR methods require bench devices and are not portable. Handheld PCR systems are under development, but more research is required to provide prepackaged reagents with longer shelf life, robustness, and efficacy (Helmus et al., 2006). Therefore, developments of high-sensitivity electronic handheld or mounted biosensors are needed to enable the cost-effective surveillance of emerging diseases as well as monitoring for biohazards and bioterrorism.

Silicon nanowires (SiNWs) have recently been developed to function as transducer for ultrasensitive biosensors and chemical sensors (Hsiao et al., 2009; Lin et al., 2008; Gao et al., 2007; Stern et al., 2007; Li et al., 2004; Patolsky et al., 2004; Cui et al., 2001). The ultrahigh sensitive detection can be attributed to their small size and large surface-to-volume ratio, enabling local charge transfers to result in a current change due to a field-effect, such as when the

* Corresponding author at: Institute of Biological Science and Technology, National Chiao Tung University, Hsinchu 300, Taiwan. Tel.: +886 3 5731983; fax: +886 3 5729288.
E-mail address: ysyang@faculty.nctu.edu.tw (Y.-S. Yang).

0956-5663/$ – see front matter © 2009 Elsevier B.V. All rights reserved.
doi:10.1016/j.bios.2009.03.014

analytical molecules bind to specific recognition molecules at the surface of the nanowire (Elfström et al., 2007). Excellent electric properties of single-crystalline silicon nanowires (single-SiNWs) for biosensing have been demonstrated (Elfström et al., 2007; Stern et al., 2007; Kamins et al., 2006; Patolsky et al., 2006; Fan and Lu, 2005; Shao et al., 2005; Chen et al., 2004; Li et al., 2004; Patolsky et al., 2004; Cui et al., 2001). However, the availability of single-SiNW FET for biological application has been seriously limited due to the difficulty in device manufacture process by either 'bottom up' (McAlpine et al., 2003; Duan et al., 2002; Cui et al., 2001) or 'top-down' (Lee et al., 2007; Li et al., 2004) lithography approaches to form monocrystalline SiNWs channels of single-SiNW FET. How to mass produce NW FET devices, control their electronic properties and reduce the cost to a reasonable range will be the key aspects for the future applications of the devices in biomedical diagnoses.

A simple and low-cost method to fabricate poly-crystalline silicon (poly-Si) NW FET for biosensing application has been previously demonstrated (Hsiao et al., 2009; Lin et al., 2008; Su et al., 2007; Su et al., 2006; Lin et al., 2005). The poly-Si sidewall spacer technique was applied for definition of the nano-scale patterns without expensive lithography tools (Su et al., 2007; Su et al., 2006; Lin et al., 2005). Most importantly, this approach is compatible with current commercial semiconductor processes and can be used to mass produce the NW FET device at low cost. The poly-SiNW FET devices showed great potential to be developed to an ultrasensitive biosensor because of their excellent electrical characteristics in aqueous solution (Lin et al., 2007). The potential of poly-SiNW FET as transducer for biosensing has been demonstrated recently using biotin and avidin/streptavidin as model system (Hsiao et al., 2009). The ultrahigh sensitivity of poly-SiNW FET for specific dopamine sensing has also been shown (Lin et al., 2008). The advantages of the poly-SiNW FET sensing device are (i) ultrasensitive and label-free, (ii) cost-effective, (iii) rapid, direct, turbid and light absorbing tolerant, and (iv) potential for developing a portable, robust, low-cost, and easy-to-handle electrical component suitable for field test and homecare use. In this report, we are trying to demonstrate that poly-SiNW FET can function as transducer for a specific and sensitive DNA biosensor. The sensing mechanism by SiNW FET can be understood in terms of the change in charge density which induces a change in electric field at the SiNW surface after hybridization (Zhang et al., 2008). The detection of HPAI virus DNA was demonstrated with a surface modified poly-SiNW FET. The result suggests that the use of poly-SiNW FET device can be an excellent choice for future biomedical application in DNA sensing.

2. Materials and methods

2.1. Materials

3-Aminopropyltriethoxysilane (APTES), sodium cyanoborohydride ($NaBH_3CN$), and ethanolamine were purchased from Sigma–Aldrich (USA). Glutaraldehyde (25%) in aqueous solution was purchased from Fluka (USA). Potassium phosphate monobasic and potassium phosphate dibasic were purchased from J.T. Baker (USA). AIV HA DNA sequences were designed based on the past researches (Wang et al., 2008; Townsend et al., 2006). All synthetic oligonucleotides were purchased from MDBio Inc. (Taiwan) including 5′-aminomodified poly-G captured DNA probe (5′-NH_2-GGG GGG GGG GGG GGG-3′), 5′-aminomodified complementary AIV H5 captured DNA probe (5′-NH_2-CAA ATC TGC ATT GGT TAT CA-3′), 5′-aminomodified complementary AIV H7 captured DNA probe (5′-NH_2-CAA ATT GAC CCA GTC AAA TTG AGT A-3′), 5′-fluorescein isothiocyanate (FITC) modified poly-C target DNA (5′-FITC-CCC CCC CCC CCC CCC-3′), AIV H5 target DNA (5′-TGA TAA CCA ATG CAG ATT TG-3′), and AIV H7 target DNA (5′-TAC TCA ATT TGA CTG GGT CAA TTT G-3′). Phosphate buffer solution (PBS) was prepared in deionized water (DIW) and its pH was adjusted to 7.0. All other solutions were prepared with DIW (resistance of water was 18.2 MΩ cm) from an ultra-pure water system (Barnstead).

2.2. Fabrication of poly-SiNW FET devices

Poly-SiNW FET devices were fabricated at the National Nano Device Laboratories (Hsinchu, Taiwan). *N*-type nano devices with two poly-Si nanowire-channels, 80 nm width and 2 μm length, were fabricated based on the poly-silicon sidewall spacer technique. This approach was compatible with current commercial semiconductor process and was previously developed by our team with special consideration for applications in aqueous solution (Hsiao et al., 2009; Lin et al., 2008; Lin et al., 2007; Su et al., 2007; Su et al., 2006; Lin et al., 2005).

2.3. Electric measurements of poly-SiNW FET

The gate potential and source/drain bias voltage were controlled with chip analyzer (Keithley 2636). Generally, in the measurement of the I_D–V_D curve, the drain current (I_D) was measured at several constant bias voltage (V_G from 5.0 to 9.0 V with a step of 1.0 V) while sweeping the V_D from 0 to 3.0 V to test the performance of poly-SiNW FET. Generally, in the measurement of the I_D–V_G curve, I_D was measured at constant bias voltage (V_D = 0.5 V) while sweeping the gate potential (V_G) from 5.0 to 10.0 V to test the poly-SiNW FET performance in aqueous solution and determine the biosensing parameters. To ensure that the device was in the same initial state, we performed a sweep started at 5.0 V bias. After the stabilized base I_D–V_G curve was obtained in PBS (10 mM, pH 7.0), the AIV target DNA in PBS (about 0.1 μl) was loaded directly on the nano device with a micro pipette. When comparing I_D–V_G curve behavior to those of controlled experiments, we noted that the biosensing tests gave the current shift at the same bias conduction. The electric response of DNA/DNA hybridization was observed as soon as the target DNA was added. It took 3 min to obtain an *I*–*V* curve and the *I*–*V* curve remained stable during the incubation. In a typical experiment, the determination of *I*–*V* curve was repeated three times to make sure that no further variation can be observed.

2.4. Immobilization of captured DNA probe on poly-SiNW FET

Immobilization of captured DNA probe on poly-SiNW surface was prepared following a three-step procedure illustrated in Fig. 1. The micro-fluidic channel, which was made with acrylic, polydimethylsiloxane (PDMS) and metal holder, was placed on top of the device to hold the aqueous solution surrounded poly-SiNW. The poly-SiNWs were firstly washed by ethanol solution to remove contaminants before 2.0% APTES ethanol solution was pumped into the microfluidic channel for 30 min to introduce amino group on the poly-SiNW surface. The device was then washed with ethanol (99.5%) three times, and heated at 120 °C for 10 min to remove the surplus ethanol. Secondly, the device surface was covered with solutions of 2.5% glutaraldehyde in 10 mM PBS (pH 7.0) and 4 mM sodium cyanoborohydride for 1 h followed by PBS wash. Finally, the 10 μM 5′-amniomodified captured DNA probe was coupled to the surface of the nanowire in PBS that contained 4 mM sodium cyanoborohydride for 1 h. The un-reacted aldehyde groups were blocked by mixing with 50 mM ethanolamine for 30 min and the modified poly-SiNW FET was washed with PBS.

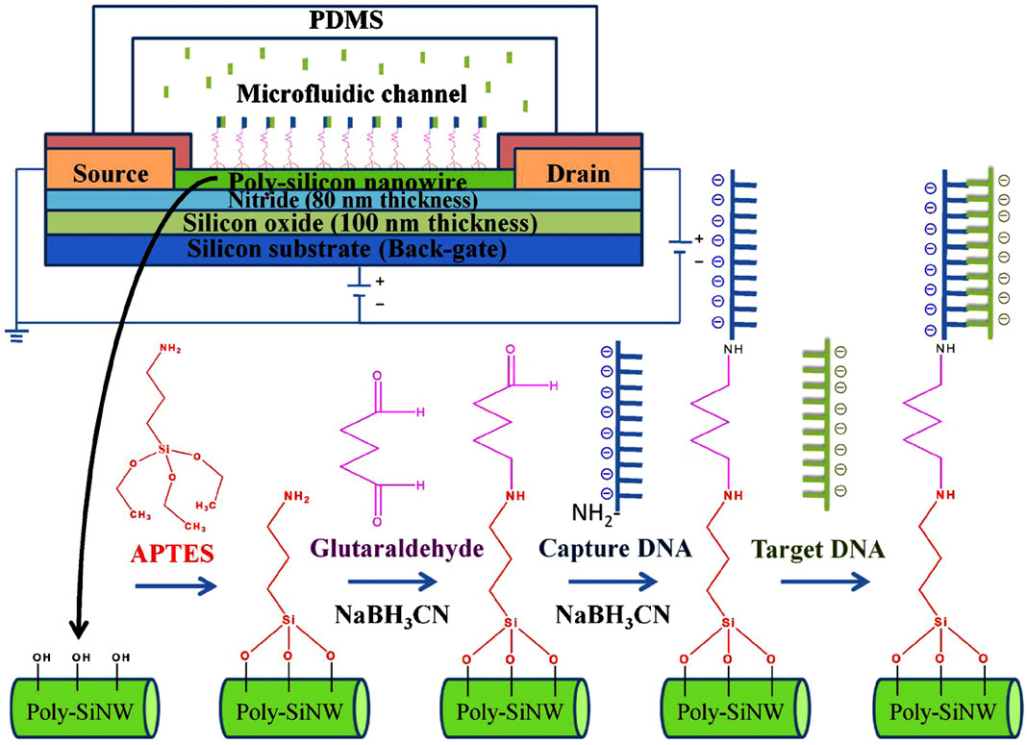

Fig. 1. Functionalization of poly-SiNW for HPAI virus DNA detection.

3. Results and discussion

3.1. Device layout and electrical characterization of poly-SiNW FET

The structure of the nano device used in this study was verified using optical and electron microscopy as shown in Fig. S1 of Supplement Information. This is an n-type poly-SiNW FET device fabricated based on our previously reported methods (Hsiao et al., 2009; Lin et al., 2008; Su et al., 2007; Su et al., 2006; Lin et al., 2005). In Fig. S1A, the optical image showed four sets of poly-SiNW FETs on the silicon wafer. The nanowire between the source and drain is invisible in Fig. S1A and is shown in the SEM image (Fig. S1B). The source and drain pads were connected to tungsten probe needles to measure the electric properties of the device at room temperature using three probes contact geometries. According to the fabrication process, each dummy-gate indirectly defined two NW channels that were connected to the source and drain pads and thus poly-SiNW FET shown in Fig. S1B contained two NWs. A significant portion of the poly-SiNW channel (an 80 nm width surface as shown in Fig. S1C) was exposed to the environment and served as the sensing site. This fabrication process (Lee et al., 2007; Li et al., 2004) is compatible with current commercial semiconductor process and thus the device can be obtained commercially in the future for biosensing and biomedical application.

The electric properties of the poly-SiNW FETs were verified with I_D–V_D, I_D–V_G, and I_G–V_G curves shown in Fig. S2 of Supplement Information. The I_D versus V_D output characteristics of a representative poly-SiNW FET were shown in Fig. S2A for V_G varying from 5.0 to 9.0 V with 1.0 V per step. The measured I_D–V_D characteristics showed that the current of the device between the source and drain was controlled effectively by the potential of the gate electrode. Typical characteristics of the poly-SiNW FET at room temperature were shown in Fig. S2B. The I_D versus V_G (from 6.0 to 9.0 V) output characteristics with V_D constant (0.5 V) exhibited excellent semiconductor FET characteristics, illustrating n-type behavior. Good device performance with high on/off current ratio (around six orders) and reasonable subthreshold swing (230 mV/dec) was achieved (Fig. S2B). In conventional poly-Si TFTs, the large amount of defect contained in the poly-Si film leads to high subthreshold slope and off-state leakage current. Owing to the tiny volume, the total defects in the nanowire channel are dramatically reduced. This feature facilitates the realization of poly-Si devices with steep subthreshold slope that is needed for application in high sensitivity biosensing. The I_D–V_G curve in aqueous solution shown in Fig. S2B was similar to that obtained in air. Our results indicate that the presence of the protection layers (100 nm wet-oxide and 80 nm nitride, Fig. S1C) can keep a low gate leakage current and this is especially important when highly sensitive transducer is required. Si substrate covered with the wet-oxide and nitride layers were used to prevent the device from liquid invasion and retain its excellent electrical characteristics and minimal leakage current between back-gate and source/drain electrode in aqueous solution (Hsiao et al., 2009).

3.2. Surface functionalization of poly-SiNW FET with DNA probe

The DNA functionalized device was monitored by fluorescent labeling (Fig. S3) using 5′-FITC modified poly-C target DNA (5′-FITC-poly-C_{target}) as the fluorescent reporter. Poly-G captured DNA probe (poly-$G_{capture}$) and non-specific captured DNA probe ($cH5_{capture}$) were functionalized on the surface of poly-SiNW FET according to the procedure diagramed in Fig. 1. Fluorescence was not observed on the surface of the device with the addition of 5′-FITC-poly-C_{target} on unmodified poly-SiNW FET under blue light excitation (Fig. S3A). Poly-$G_{capture}$ cannot be linked to the silicon oxide surface in the absence of glutaraldehyde, and thus the fluorescence was not observed in Fig. S3B either. Clear distinction in fluorescence was observed between Fig. S3C and D. H5 captured DNA probe ($cH5_{capture}$) modified device did not give fluorescence (Fig. S3C). Only the device functionalized with specific poly-$G_{capture}$ (Fig. S3D) gave the expected fluorescent upon hybridization with 5′-FITC-

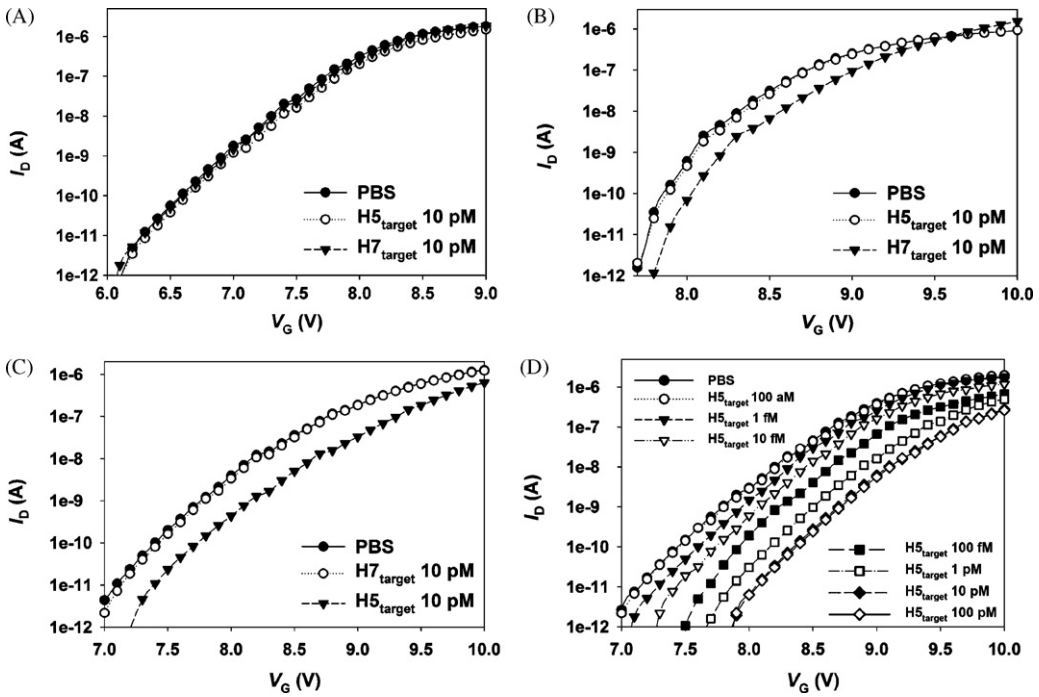

Fig. 2. Electric responses of functionalized poly-SiNW FET to specific AIV HA target DNA (HA_{target}) in aqueous solution. (A) I_D–V_G curves obtained from unmodified poly-SiNW FET. (B) I_D–V_G curves obtained from H7 captured DNA probe ($cH7_{capture}$) functionalized poly-SiNW FET device. (C) I_D–V_G curves obtained from $cH5_{capture}$ functionalized poly-SiNW FET device. (D) Titration curves of $cH5_{capture}$ functionalized poly-SiNW FET device by $H5_{target}$. A constant V_D was set at 0.5 V for all the electric measurement.

poly-C_{target} under blue light excitation. As shown in Fig. S3D, the nitride layer was found to be non-fluorescent because only the surface of silicon oxide could be modified with APTES. For the functionalization of H5 and H7 captured DNA probe on the poly-SiNW, the PDMS micro-fluidic channel was used to hold the aqueous solution surrounded poly-SiNW (top Fig. 1). The similar procedures were used to functionalize poly-SiNW with biotin and 4-carboxyphenylboronic acid for the specific detection of avidin/streptavidin and dopamine, respectively (Hsiao et al., 2009; Lin et al., 2008).

3.3. Electric responses from specific DNA/DNA interactions on poly-SiNW FET

Sensitivity and specificity of functionalized poly-SiNW FET for biosensing DNA/DNA interactions are shown in Fig. 2. The increase in negative charges resulted from hybridization between target DNA and complementary captured DNA probe can greatly affect the surface conductivity of SiNW FET. For an n-type NW FET, a decrease of the current will be expected when negative charges were introduced on its sensing surface. Controlled experiments with naked (unmodified) poly-SiNW FET are shown in Fig. 2A. The I_D–V_G curves remained unchanged in PBS buffer and in the presence of either $H5_{target}$ or $H7_{target}$ indicated that the electric property of poly-SiNW FET was stable in the presence of non-interacting charged molecules, which may exist in a variety of biological samples. Since only charges on the SiNW surface can cause significant changes of the I_D–V_G curves, Fig. 2A demonstrated that there was little non-specific binding between DNA and naked poly-SiNW FET. Similar results were observed in Fig. S4A and B. The poly-SiNW FET devices functionalized with only APTES (Fig. S4A) and APTES plus glutaraldehyde (Fig. S4B), respectively, did not give variation in I_D–V_G curves in the presence of either $H5_{target}$ or $H7_{target}$. These results indicate that non-specific binding of target DNA to APTES and glutaraldehyde modified SiNW did not occur.

The selectivity of functionalized poly-SiNW FET is shown in Fig. 2B and C. Two captured DNAs, $cH7_{capture}$ and $cH5_{capture}$, were respectively immobilized on the surface of poly-SiNW FETs according to Fig. 1. The electric responses of the functionalized poly-SiNW FETs were demonstrated to be dependent on the presence of $H5_{target}$ and $H7_{target}$ DNAs. For the $cH7_{capture}$ functionalized poly-SiNW FET (Fig. 2B), I_D–V_G curves were indistinguishable in PBS and in the presence of $H5_{target}$. However, a momentous current decrease was observed in the presence of 10 pM $H7_{target}$. This observation strongly indicated that only specific DNA/DNA interaction can occur on poly-SiNW FET surface. Similar observation is shown in Fig. 2C. The $cH5_{capture}$ functionalized poly-SiNW FET gave similar I_D–V_G curves in the PBS and in the presence of $H7_{target}$. The expected change of electric response was observed in the presence of 10 pM $H5_{target}$. The results strongly suggested that only specific HA_{target} binds to the $cHA_{capture}$ modified poly-SiNW surface and induces change of I_D–V_G curve. This also indicated that a sensitive and specific sensing device for the diagnosis of AIV infection can be achieved.

The lowest detectable concentration and detection range of $H5_{target}$ with $cH5_{capture}$ modified poly-SiNW FET are shown in Fig. 2D. Concentration-dependent electronic responses were observed for $H5_{target}$ concentration increasing from 1 fM to 10 pM. No significant influence on the current was evidenced for concentrations >10 pM. This observation further confirmed that the change of current in I_D–V_G curve was specifically affected by the interaction between $H5_{target}$ and $cH5_{capture}$ on the SiNW surface. The I_D–V_G curve remained constant after saturation even when much higher concentration of $H5_{target}$ (100 pM) was added. As depicted in Fig. 3, the changes of logarithmic drain current ($\Delta \log I_D$) increased with $H5_{target}$ concentration ranging from 1 fM to 10 pM. According to the approximate volume of $H5_{target}$ used (0.1 μl), the number of $H5_{target}$ molecules were about 60 at 1 fM. This number is lower than that of our previous report (Lin et al., 2008) for dopamine detection (about 600 molecules). This result is expected because

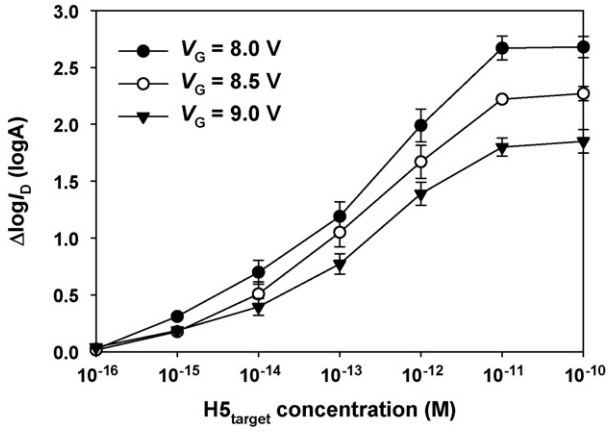

Fig. 3. The changes of logarithmic drain current ($\Delta \log I_D$) of $cH5_{capture}$ functionalized poly-SiNW FET with $H5_{target}$ at different concentrations. The log I_D was obtained for different gate voltages: 8.0, 8.5, and 9.0 V, respectively. The logarithmic drain current obtained in PBS was used as background current. The reaction condition is described in Fig. 2. Each data was the average of three measurements.

dopamine can produce only one negative charge per molecule on poly-SiNW surface (Lin et al., 2008) while each hybridization between $H5_{target}$, a 20-mer DNA, and $cH5_{capture}$ produces about 20 extra negative charges. This indicates that the sensitivity of DNA sensing can be further improved if the target DNA contains longer sequence.

It is interesting to point out that the induced change of current (I_D) following DNA hybridization was dependent on the applied gate voltage (V_G). As shown in Fig. 2B–D, the smaller I_D change was observed at higher V_G. Fig. 3 gives the changes of I_D for three different V_G. This observation provides us important information for the future development of the poly-SiNW FET for a variety of biological sensing experiments. The exact origin for this phenomenon is not clear at this stage. It might be caused by the high parasitic source/drain resistance of the poly-SiNW devices which tends to reduce the effective field inside the channel. Another possible explanation is the channel heating effect which tends to reduce the carrier mobility. In the future, the biosensing measurement will be done at a specific V_G to obtain certain electric variations under different experimental conditions. In a few cases, there were disparities in the *I–V* characteristics of the devices measured in PBS, which were attributed to the performance fluctuation, mainly due to the use of thick gate dielectric and non-regular cross-sectional shape of the NWs (Fig. 2). This variation can be eliminated or greatly improved in the future when the procedures for the poly-SiNW FET fabrication become standardized. At present, the V_G dependent induced I_D changes gave an extra mean to distinguish the I_D changes caused by non-homogeneity of the device or by the DNA/DNA hybridization. The disparities in *I–V* characteristics between devices do not affect the biosensing event, which was determined according to the electric changes in each device.

This is the first report for label-free detection of HPAI virus DNA at fM concentration. Compared to other methods for the label-free detection of DNA, surface-plasma resonance has the lowest detectable concentration reported at 0.677 pM for peptide nucleic acid–DNA hybridization (Endo et al., 2005). Quartz-crystal microbalance has the lowest detectable concentration reported at 1 pM for DNA/DNA hybridization (Lu et al., 2007). The lowest detectable concentration and detection range shown in Figs. 2 and 3 were comparable to the similar scheme using single-SiNW FET that required a costly fabrication substrate (Gao et al., 2007). In addition to its ultrahigh sensitivity as biosensing transducer, poly-SiNW FET has other advantages in fabrication process (Hsiao et al., 2009; Lin et al., 2008; Lin et al., 2007; Lin et al., 2005) for biomedical application, which include (i) high uniformity and reproducibility, (ii) high yield, and (iii) excellent scalability and manufacturability. It is possible to produce SiNW FET of both low- and high-multiplexing capabilities and permits direct integration with electrical readout circuits. The unique aspect of this development is the incorporation of additional technology to make the method usable in remote locations, including real-time secure communications.

4. Conclusions

We have demonstrated for the first time that semiconducting poly-SiNW FET could be developed to a highly specific sensor for HPAI virus DNA with sensitivity in the fM concentration range. Throughout the fabrication of the poly-SiNW FET, no expensive lithography tools were needed for definition of nano-scale patterns. Our results indicate that fabrication of poly-SiNW FET for sensitive and specific biosensing device can be achieved using commercially available procedures. This would be of great scientific and commercial values and may open the door to real-time molecular diagnostics and direct surveillance of infection diseases.

Acknowledgement

This research is financially supported by National Science Council, Taiwan (97-2321-B-009-001).

Appendix A. Supplementary data

Supplementary data associated with this article can be found, in the online version, at doi:10.1016/j.bios.2009.03.014.

References

Chen, R.J., Choi, H.C., Bangsaruntip, S., Yenilmez, E., Xiaowu, T., Wang, Q., Chang, Y.L., Dai, H.J., 2004. J. Am. Chem. Soc. 126, 1563–1568.
Cui, Y., Wei, Q., Park, H., Lieber, C.M., 2001. Science 293, 1289–1292.
Deregt, D., Furukawa-Stoffer, T.L., Tokaryk, K.L., Pasick, J., Hughes, K.M., Hooper-McGrevy, K., Baxi, S., Baxi, M.K., 2006. J. Virol. Methods 137, 88–94.
Duan, X., Huang, Y., Lieber, C.M., 2002. Nano Lett. 2, 487–490.
Durham, S., 2003. Agric. Res. Mag. 51, 9.
Elfström, N., Juhasz, R., Sychugov, I., Engfeldt, T., Eriksson Karlström, A., Linnros, J., 2007. Nano Lett. 7, 2608–2612.
Endo, T., Kerman, K., Nagatani, N., Takamura, Y., Tamiya, E., 2005. Anal. Chem. 77, 6976–6984.
Fan, Z., Lu, J.G., 2005. Appl. Phys. Lett. 86, 123510.
Gao, Z., Agarwal, A., Trigg, A.D., Singh, N., Fang, C., Tung, C.H., Fan, Y., Buddharaju, K.D., Kong, J., 2007. Anal. Chem. 79, 3291–3297.
Helmus, M.N., Gammel, P., Allen, F., Migliorato, P., 2006. Am. Lab. 38, 34–38.
Hsiao, C.Y., Lin, C.H., Hung, C.H., Su, C.J., Lo, Y.R., Lee, C.C., Lin, H.C., Ko, F.H., Huang, T.Y., Yang, Y.S., 2009. Biosens. Bioelectron. 24, 1223–1229.
Kamins, T.I., Sharma, S., Yasseri, A.A., Li, Z., Straznicky, J., 2006. Nanotechnology 17, S291–S297.
Lee, K.N., Jung, S.W., Kim, W.H., Lee, M.H., Shin, K.S., Seong, W.K., 2007. Nanotechnology 18, 445302.
Li, Z., Chen, Y., Li, X., Kamins, T.I., Nauka, K., Williams, R.S., 2004. Nano Lett. 4, 245–247.
Lin, C.H., Hsiao, C.Y., Hung, C.H., Lo, Y.R., Lee, C.C., Su, C.J., Lin, H.C., Ko, F.H., Huang, T.Y., Yang, Y.S., 2008. Chem. Commun. 44, 5749–5751.
Lin, H.C., Lee, M.H., Su, C.J., Huang, T.Y., Lee, C.C., Yang, Y.S., 2005. IEEE Electron Device Lett. 26, 643–645.
Lin, H.C., Su, C.J., Hsiao, C.Y., Yang, Y.S., Huang, T.Y., 2007. Appl. Phys. Lett. 91, 202113.
Lodes, M.J., Suciu, D., Elliott, M., Stover, A.G., Ross, M., Caraballo, M., Dix, K., Crye, J., Webby, R.J., Lyon, W.J., Danley, D.L., McShea, A., 2006. J. Clin. Microbiol. 44, 1209–1218.
Lu, W., Lin, L., Jiang, L., 2007. Biosens. Bioelectron. 22, 1101–1105.
McAlpine, M.C., Friedman, R.S., Jin, S., Lin, K.H., Wang, W.U., Lieber, C.M., 2003. Nano Lett. 3, 1531–1535.
Patolsky, F., Zheng, G., Hayden, O., Lakadamyali, M., Zhuang, X., Lieber, C.M., 2004. Proc. Natl. Acad. Sci. U.S.A. 101, 14017–14022.
Patolsky, F., Zheng, G., Lieber, C.M., 2006. Nanomedicine 1, 51–65.
Shao, M.W., Shan, Y.Y., Wong, N.B., Lee, S.T., 2005. Adv. Funct. Mater. 15, 1478–1482.
Stern, E., Klemic, J.F., Routenberg, D.A., Wyrembak, P.N., Turner-Evans, D.B., Hamilton, A.D., LaVan, D.A., Fahmy, T.M., Reed, M.A., 2007. Nature 445, 519–522.
Su, C.J., Lin, H.C., Huang, T.Y., 2006. IEEE Electron Device Lett. 27, 582–584.

Su, C.J., Lin, H.C., Tsai, H.H., Wang, T.M., Huang, T.Y., Ni, W.X., 2007. Nanotechnology 18, 215205.
Townsend, M.B., Dawson, E.D., Mehlmann, M., Smagala, J.A., Dankbar, D.M., Moore, C.L., Smith, C.B., Cox, N.J., Kuchta, R.D., Rowlen, K.L., 2006. J. Clin. Microbiol. 44, 2863–2871.
Tsuda, Y., Sakoda, Y., Sakabe, S., Mochizuki, T., Namba, Y., Kida, H., 2007. Microbiol. Immunol. 51, 903–907.
Wang, L.C., Pan, C.H., Severinghaus, L.L., Liu, L.Y., Chen, C.T., Pu, C.E., Huang, D., Lir, J.T., Chin, S.C., Cheng, M.C., Lee, S.H., Wang, C.H., 2008. Vet. Microbiol. 127, 217–226.
Wu, C., Cheng, X., He, J., Lv, X., Wang, J., Deng, R., Long, Q., Wang, X., 2008. J. Virol. Methods 148, 81–88.
Zhang, G.J., Zhang, G., Chua, J.H., Chee, R.E., Wong, E.H., Agarwal, A., Buddharaju, K.D., Singh, N., Gao, Z., Balasubramanian, N., 2008. Nano Lett. 8, 1066–1070.